CHEMISTRY
A EUROPEAN JOURNAL

DOI: 10.1002/chem.200501494

Paramagnetic Properties of the Halide-Bound Derivatives of Oxidised Tyrosinase Investigated by ^{1}H NMR Spectroscopy

Armand W. J. W. Tepper,[a] Luigi Bubacco,[b] and Gerard W. Canters*[c]

Abstract: The ^{1}H NMR relaxation characteristics of the histidines in the oxidised type-3 copper site of tyrosinase (Ty_{met}) from the bacterium *Streptomyces antibioticus* in the halide-bound forms ($Ty_{met}X$ with $X = F^-$, Cl^-, Br^-) have been determined and analysed. The ^{1}H NMR spectra of the $Ty_{met}X$ species display remarkably sharp, well-resolved, paramagnetically shifted ^{1}H signals, which originate from the protons of the six His residues coordinated to the two Cu^{II} ions in the type-3 centre. From the temperature-dependence of the ^{1}H paramagnetic shifts the following values for the exchange-coupling parameter $-2J$ were determined: 260 ($Ty_{met}F$), 200 ($Ty_{met}Cl$) and 162 cm^{-1} ($Ty_{met}Br$). The ^{1}H T_1 relaxation is dipolar in origin and correlates with the Cu–H distances. Electronic relaxation times τ_S derived from the ^{1}H T_1 data amount to about 10^{-11} s and follow the order $Ty_{met}F > Ty_{met}Cl > Ty_{met}Br$. They are two orders of magnitude shorter than the τ_S values reported for mononuclear copper systems, in accordance with the sharpness of the ^{1}H signals. The results corroborate the Cu_2 bridging mode of the halide ions. On the basis of the measured hyperfine interaction constants for the ligand histidine nuclei, it is concluded that 70–80% of the spin density in the excited triplet state resides on the two copper ions and the bridging atoms.

Keywords: copper · electronic structure · enzymes · NMR spectroscopy · relaxation

Introduction

Enzymes and proteins with a dinuclear type-3 Cu site function as oxygen carriers or phenol and catechol oxidases in living organisms. While the three-dimensional structures of some members of this family have been determined (vide infra), the structure of tyrosinase (Ty) and its enzyme mechanism have remained largely unknown.[1] This work reports on a study of the nuclear and electronic relaxation properties of the halide-bound derivatives of oxidized tyrosinase from *Streptomyces antibioticus*. It shows how the paramagnetic shifts provide information on the spin-density distribution in the active site and how the relaxation properties can be used to derive structural information on the active centre and to shed light on the mechanisms responsible for the sharpness of the paramagnetic ^{1}H spectra of halide-bound tyrosinase.

Ty catalyses the ortho-hydroxylation of monophenols and the subsequent oxidation of the reaction product to the corresponding quinone under concomitant reduction of dioxygen to water. The quinones are precursors in the synthesis of melanin pigments. Ty occurs widely in nature and can be found in organisms ranging from bacteria to man. The type-3 copper centre in the catalytic site of the enzyme comprises two closely spaced copper ions (Cu–Cu distance ~3–4 Å) each coordinated by three protein-derived His ligands.[2,3] The type-3 site can be further found in the catechol oxidases (COs) and the hemocyanins (Hcs). These proteins are responsible for the oxidation of diphenols in plants and oxygen storage and oxygen transport in arthropods and molluscs, respectively. Crystal structures are available for one CO[4] and several Hcs.[5–7] The type-3 centres of Tys, Hcs, and COs appear remarkably similar as demonstrated by their unique spectroscopic signatures and the conserved amino acid sequences of their Cu_2 binding domains.

[a] Dr. A. W. J. W. Tepper
Leiden Institute of Chemistry
Gorlaeus Laboratories, Leiden University
Einsteinweg 55, 2333 CC, Leiden (The Netherlands)
[b] Dr. L. Bubacco
Department of Biology, University of Padua
Via Trieste 75, 30121 Padua (Italy)
[c] Prof. Dr. G. W. Canters
Leiden Institute of Chemistry
Gorlaeus Laboratories, Leiden University
Einsteinweg 55, 2333 CC, Leiden (The Netherlands)
Fax: (+31) 71-527-4349
E-mail: canters@chem.leidenuniv.nl

Supporting information for this article is available on the WWW under http://www.chemeurj.org/ or from the author.

Ty can exist in several forms, including a) the reduced [Cu^{I} Cu^{I}] form (Ty_{red}), b) the oxygenated [Cu^{II}–O_2^{2-}–Cu^{II}] form (Ty_{oxy}), and c) the oxidised [Cu^{II}–R–Cu^{II}] form (Ty_{met}). In Ty_{met}, the two $S = {}^1/_2$ copper ions are antiferromagnetically coupled through spin superexchange mediated by a Cu_2 bridging ligand.[1] This results in a diamagnetic singlet $S = 0$ ground state and a paramagnetic triplet $S = 1$ excited state with a singlet–triplet energy splitting of $-2J$. At low temperature (i.e. when $k_BT \ll -2J$), only the diamagnetic $S = 0$ ground state is populated, rendering the Ty_{met} site devoid of an EPR signal.[1]

NMR spectroscopy can be a powerful tool in the study of paramagnetic proteins. In general, paramagnetism induces large shifts and relaxation enhancements of nuclei in close vicinity to the paramagnetic centre, quantities that both contain information concerning the structure of and the spin-distribution over the active site.[8] The applicability of the NMR technique depends on the electronic relaxation characteristics of the paramagnetic centre. When electron relaxation is fast (e.g. low-spin Fe^{3+}, Ni^{2+}, or high-spin Co^{2+}) good resolution is usually obtained. In systems in which electron relaxation is slow (e.g. Cu^{2+}), the signals of nuclei of coordinating ligands are often broadened beyond detection.

Several *dinuclear* Cu^{II} compounds (e.g.[9–14]), as well as Cu^{2+}-substituted aminopeptidase,[9] appear to give relatively sharp NMR signals. As in the case of Ty, these Cu_2 compounds carry two closely spaced magnetically coupled copper atoms. If the magnetic exchange interaction $-2J$ is of the order of k_BT, the paramagnetic $S = 1$ level is only partially occupied, reducing both the paramagnetic shifts in the NMR spectrum and the effect of paramagnetic relaxation. Partial occupation has been invoked to qualitatively explain why the signals in the ^{1}H NMR spectra of a number of biomimetic binuclear copper compounds are relatively sharp.[15] In a number of cases, however, signals appeared much sharper than could be expected on the basis of a reduction in paramagnetism. In these cases the sharpening was proposed to be connected to a shortening of the electron spin relaxation time, τ_S, of the paramagnetic state.[9,15] Apparently, the coupling of the two Cu^{2+} ions provides for spin-relaxation pathways that are unavailable to mononuclear Cu sites.[12,15–18]

Also for tyrosinase the paramagnetically affected ^{1}H NMR signals appear remarkably sharp, especially in the presence of halides.[2,3] ^{1}H NMR studies have demonstrated that Ty_{met} contains a classical type-3 copper centre with the two copper ions in the active site each coordinated by three histidines through the N^{ε} atoms.[2,3] Furthermore, from paramagnetic NMR and kinetic studies,[3,19] it was tentatively concluded that halides bridge the two copper ions in the Ty_{met} active site, replacing the Cu_2 bridging hydroxide that is present in native Ty_{met}.

Since the paramagnetically shifted signals in the Ty_{met} ^{1}H NMR spectrum provide a sensitive fingerprint of the active site,[3,20,21] NMR spectroscopy can be used to monitor ligand binding to obtain binding constants, for example. Depending on the relaxation characteristics of the system, T_1 and T_2 relaxation data may also be used to estimate distances from the copper to the resonating nucleus to gain information on the coordination geometry of bound exogenous ligands. To pursue such an approach, the relaxation characteristics of the system should be known.

Here we report on a relaxation analysis of Ty_{met} in its halide-bound forms. Values for the singlet-triplet spacing energy $-2J$ were determined. Using the T_1 relaxation data and HisH–Cu distances derived from crystal structures, estimates for the electronic relaxation times τ_S were obtained. The results provide evidence for a bridging mode of halide ions. Furthermore, it is shown that fast electronic relaxation is responsible for the sharpness of the paramagnetically affected signals in tyrosinase.

Results

^{1}H NMR spectra: Figure 1 shows the 600-MHz ^{1}H NMR spectra, recorded at pH 6.80 and 4 °C, of the halide-bound Ty_{met} derivatives between $\delta = 55$ and 10 ppm.[2,3] For Ty_{met}F (Figure 1A) and Ty_{met}Cl (Figure 1B), the paramagnetically shifted resonances have been assigned based on H_2O/D_2O exchange experiments, intraresidue NOE patterns, and T_1 relaxation data.[2,3] The sharp, solvent-exchangeable signals could be assigned to the N^{δ} protons of the coordinating histidine residues, while the broader signals derive from the C^{ε} and C^{δ} protons of the histidines. Furthermore, the NOE patterns in the spectrum of Ty_{met}Cl were used to identify the coupling of each of the six sharp N^{δ} proton signals with a C^{ε} proton signal, thereby characterising each histidine residue in the $(Cu–His_3)_2$ coordination sphere as indicated in Figure 1B.[2] In the case of Ty_{met}F (Figure 1A), the detection of NOE signals is complicated by signal overlap and by the fast T_1 relaxation (see below). Four out of the six expected NOE connectivities in the Ty_{met}F species could be detected[3] as presented in Figure 1A.

Magnitude of the exchange coupling: The magnitude of the exchange coupling ($-2J$) between the two unpaired electrons of the Cu^{II} ions can be estimated by investigating the temperature dependence of the chemical shifts.[2,12,13,29,30] These were measured for all resolved paramagnetically shifted signals in the Ty_{met}X species in the 279–300 K range. The Curie plots for the shift data are presented in Figure 2. The data were analysed by global fitting to Equation (1) (Experimental Section), resulting in a single value for $-2J$ (Table 1) and a value for the contact coupling constant A_M for each signal (Table 2). In the cases of Ty_{met}F and Ty_{met}Br, one signal showed erroneous temperature dependence (marked with open symbols in Figure 2) and we did not include the shift data of these signals in the fitting procedure. Also for the protons with a small contact shift the quality of the fit is not optimal. This may be related to the use of the uniform diamagnetic correction of 8 ppm to the chemical shift, which in actuality may vary between 4 and 12 ppm. Es-

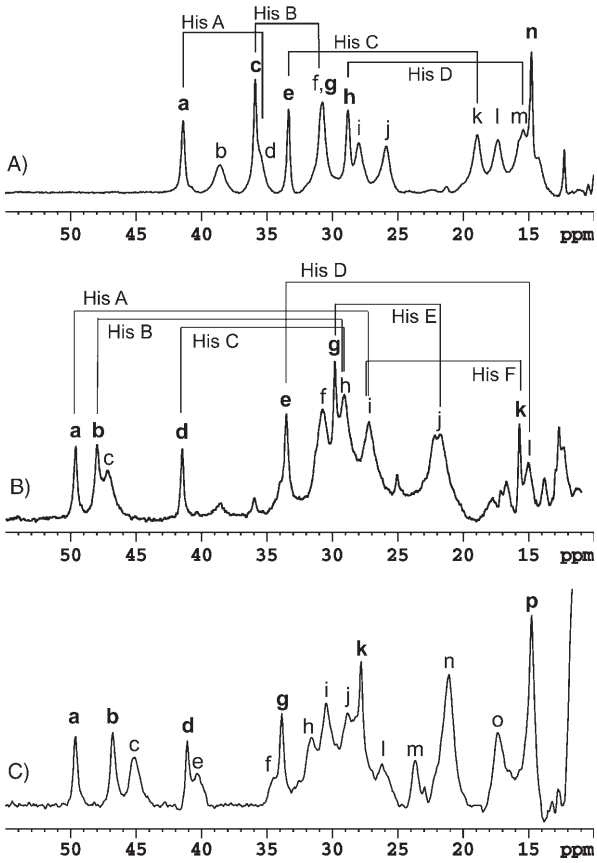

Figure 1. Paramagnetic ^{1}H NMR spectra of the halide-bound derivatives of oxidised tyrosinase (Ty_{met}). A) $Ty_{met}F$, fluoride-bound; B) $Ty_{met}Cl$, chloride-bound; C) $Ty_{met}Br$, bromide-bound. The sharp signals assigned to the N^{δ} protons of the coordinating His residues are labelled in *bold type italics*, while the broader signals assigned to the coordinating His C^{δ} and C^{ε} protons are labelled in normal font. For $Ty_{met}F$ and $Ty_{met}Cl$, the detected NOE connectivities between His N^{δ} and His C^{ε} protons are also shown. The A–D labels in (A) do not correspond to the A–F labels in (B).

pecially when the contact shift is small, a change in the diamagnetic correction may result in a seemingly aberrant slope of the Curie plot.

T_1 relaxation data: We have measured T_1 values for $Ty_{met}F$ and $Ty_{met}Br$. The data are presented in Table 2 together with previously derived data for the chloride-bound species.[2] Mono-exponential relaxation behaviour is observed for all broad signals that consist of multiple overlapping resonances (as judged by signal integration), indicating that the resonances making up the total signal share similar T_1 relaxation times. The narrow widths and relatively long T_1s (see below) of the $N^{\delta}H$ signals allowed for measurement of the T_1 values of the latter despite the occasional overlap with broader $C^{\delta,\varepsilon}H$ signals. The T_1 could not be accurately estimated for signal *g* in the spectrum of $Ty_{met}F$ and signal *p* in the spectrum of $Ty_{met}Br$, in which a sharp $N^{\delta}H$ signal is exactly superimposed on a broad His $C^{\delta,\varepsilon}H$ signal. For $Ty_{met}F$, the T_1 values of the broad signals (from the His C^{δ} and C^{ε} protons) were measured in D_2O. Under these conditions the $N^{\delta}H$ signals are not observed, which allows for a more accurate measurement of the T_1 of the remaining signals.

For the $Ty_{met}X$ species, the longitudinal relaxation times divide into two distinct groups: the His $N^{\delta}H$ signals all share similar T_1 values (14–18, 17–27 and 26–32 ms for the F^-, Cl^- and Br^- derivatives, respectively), as do the His-CH signals (2–4, 4–7 and 6–10 ms in the same order). There is no correlation between the determined coupling constants and T_1 relaxation times, showing that contact relaxation does not have a dominant effect on relaxation rates.

Mechanism of T_1 relaxation: In the present case molecular tumbling is slow (rotational correlation time on the order of 15–20 ns) and the correlation time for dipolar relaxation is dominated by the electronic relaxation time, $\tau_D \approx \tau_S$. Since $\omega_S\tau_S \gg 1$, contact relaxation will not significantly contribute to the T_1.[31] Also, Curie relaxation will not significantly contribute to T_1 because $\omega_I^2\tau_R^2 \gg 1$ (see [Eq. (6)], Experimental Section). Thus, the paramagnetic T_1 values are essentially dipolar in origin, which is in line with the conclusion in the previous paragraph.

Correlation of T_1s with Cu–H distances: From the crystal structures of type-3 copper proteins it appears that the six His residues making up the conserved coordination sphere of the Cu site are nearly equivalent in terms of His proton–metal distances. This is illustrated by Figure 3 in which a histogram is shown of the distances between the His N^{δ}, C^{ε}, and C^{δ} protons and the coordinated copper atom as observed in the crystal structures of *Limulus polyphemus* Hc (PDB entries 1OXY and 1 LL1),[6] *Octopus dofleini* Hc (PDB entry 1 JS8),[5] and *Ipomoea batata* CO (PDB entries 1BT3 and 1BT1)[4] either in the oxidised or the oxygenated form. The

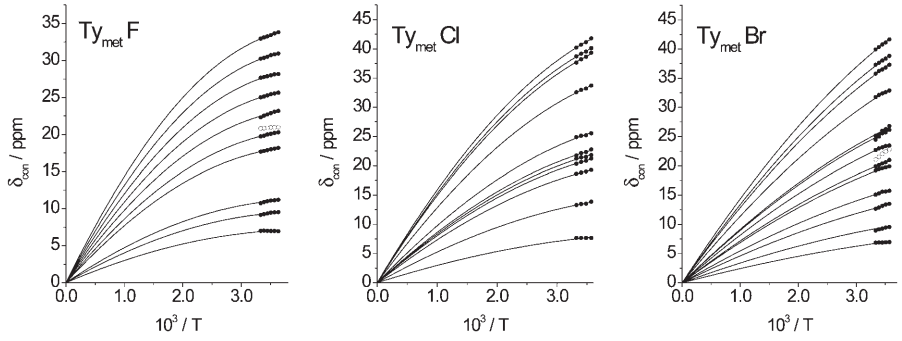

Figure 2. Curie plots for the paramagnetic shifts of $Ty_{met}F$, $Ty_{met}Cl$, and $Ty_{met}Br$. The solid lines represent fits to the data using Equation (1) with $-2J = 260\ cm^{-1}$ ($Ty_{met}F$), $200\ cm^{-1}$ ($Ty_{met}Cl$), and $162\ cm^{-1}$ ($Ty_{met}Br$). Data represented by open symbols were not included in the fitting procedure (see text).

Table 1. The exchange coupling parameter $-2J$, average T_1 values and estimated electronic relaxation times τ_S for the different halide-bound species.

Species	$-2J$ [a] [cm^{-1}]	Average T_1[b] $C^{\delta,\varepsilon}H$ [ms]	Average T_1[b] $N^{\delta}H$ [ms]	T_1 $N^{\delta}H$/ T_1 $C^{\delta,\varepsilon}H$	τ_S calcd $C^{\delta,\varepsilon}H$[c] [$\times 10^{-11}$ s]	τ_S calcd $N^{\delta}H$[c] [$\times 10^{-11}$ s]
$Ty_{met}F$	261 ± 6	2.6 ± 0.7	16 ± 3	6 ± 2	3 ± 1	5 ± 1
$Ty_{met}Cl$	200 ± 10	5.3 ± 0.9	23 ± 4	4 ± 1	1.0 ± 0.2	3 ± 1
$Ty_{met}Br$	162 ± 11	8.0 ± 1.5	29 ± 3	4 ± 1	0.6 ± 0.1	2 ± 1

[a] Values for $-2J$ were estimated on the basis of the temperature dependence of signal paramagnetic shifts and Equation (1) (see Figure 2). [b] The average T_1 values are based on the values listed in Table 2. [c] The values for τ_S were estimated on the basis of Equation (2) using the determined values for $-2J$, the average T_1 values and the average Cu–H distances found in type-3 copper proteins (Figure 3). The error margins reported for τ_S reflect the uncertainty in r and in the experimental T_1 values; See also footnote.[32] nd: values not determined.

Table 2. Shifts, coupling constants, and T_1 values of the paramagnetically affected ^{1}H signals of the halide-bound $Ty_{met}X$ species as measured (T_1 and δ) at 4 °C, pH 6.80, and 600 MHz field strength.

Signal	$Ty_{met}F$			$Ty_{met}Cl$			$Ty_{met}Br$		
	δ[a] [ppm]	A_M/h[b] [MHz]	T_1 [ms]	δ[a] [ppm]	A_M/h[b] [MHz]	T_1 [ms]	δ[a] [ppm]	A_M/h[b] [MHz]	T_1 [ms]
a	*41.3*	*2.02*	*13.8*	*49.6*	*2.18*	*23.6*	*49.4*	*1.94*	*30.2*
b	38.6	1.85	1.8[c]	*47.9*	*2.10*	*16.9*	*46.6*	*1.81*	*25.8*
c	*35.9*	*1.69*	*14.8*	47.2	2.05	6.6[c]	45.1	1.74	7.1
d	35.6	nd	1.9[c]	*41.4*	*1.76*	*26.5*	*40.7*	*1.54*	*30.9*
e	*33.3*	*1.53*	*18.3*	*33.5*	*1.34*	*18.7*	40.2	nd	10.1
f	30.7	1.38	3.2[c]	30.7	1.19	5.5[c]	35.0	1.34	7.9
g	*30.7*	*1.38*	*nd*	*29.7*	*1.15*	*26.7*	*34.3*	*1.21*	*26.3*
h	*28.8*	*1.26*	*15.3*	29.1	1.11	5.6[c]	31.3	1.11	10.4
i	28.0	1.21	3.0[c]	27.1	1.01	4.7[c]	30.6	1.05	6.7
j	25.8	1.08	2.8[c]	21.9	0.72	4.3[c]	28.9	0.97	9.0
k	19.0	0.67	3.8[c]	*15.6*	*0.41*	*24.5*	*27.7*	*0.93*	*32.2*
l	17.3	0.57	2.4[c]				26.0	nd	7.3
m	15.4	nd	2.1[c]				23.8	0.74	9.2
n	*14.9*	*0.42*	*16.5*				21.1	0.62	6.1
o							17.2	0.44	6.3
p							*14.8*	*0.33*	*nd*

[a] See Figure 1 for signal labelling. The data for the His N^{δ} protons are presented in italic font; the data for the His His C^{δ} and C^{ε} protons are presented in normal font. nd: values not determined. [b] Determined from global fit of the paramagnetic shifts versus $1/T$ (see Equation (1), Figure 2, and text). [c] Determined in D_2O. Based on the outcome of the global fit analysis, the statistical errors of the A_M/h values are less than 5%. Owing to the uncertainty in the diamagnetic correction and the neglect of a possible pseudocontact contribution to the paramagnetic shift (see text), the systematic contribution to the error may reach up to 15% for the signals with small shifts.

distances between the N^{δ} protons and Cu all amount to about 5.1 Å ($\pm$0.2 Å), while the C^{ε} and C^{δ} protons occur at distances of about 3.4($\pm$0.3 Å). There is no significant difference between the average distances obtained for the C^{ε} and the C^{δ} protons. Thus, since T_1 is predominantly dipolar in origin, the overall relaxation characteristics should be similar for equivalent His protons, as is indeed observed for the $Ty_{met}X$ species ($N^{\delta}H$ T_1s in one class, $C^{\delta,\varepsilon}H$ T_1s in another class; see Table 1).

Since detailed information on the spin-density distribution is lacking, we shall use, in the following, the point-dipolar approximation to analyse the relaxation data and to obtain a) an estimate for τ_S and b) its variation along the series $Ty_{met}F$, $Ty_{met}Cl$, and $Ty_{met}Br$.

According to the point-dipolar approximation, the T_1 values obtained for the N^{δ} protons and the C^{ε} and C^{δ} protons are in the ratio of the corresponding electron–nuclear distances to the sixth power, that is, $(r_{Cu-NH})^6/(r_{Cu-CH})^6$, which amounts to 10 ± 5 and deviates by a factor of two to three from the experimental ratios (Table 1, fifth column). The latter observation illustrates that the point-dipolar approximation in our case can only be used for qualitative estimates.[32]

Electronic relaxation times: A crude estimate for the electronic relaxation time τ_S can be obtained from the X-ray Cu–H distances (see above and Figure 3) and the experimental T_1 and $-2J$ values with the use of Equation (2) (see Experimental Section). The calculated values are presented in Table 1. By applying Equation (2), the total unpaired spin density is assumed to be located at the Cu_2 centre, which leads to a calculated correlation time that is slightly too large,[32] an effect that is more pronounced for the N^{δ} τ_S correlation times, as is observed (Table 1). Furthermore, it is observed that τ_S increases in the order $Ty_{met}Br < Ty_{met}Cl < Ty_{met}F$.

Mechanism of T_2 transversal relaxation: To analyse the mechanism of the transversal relaxa-

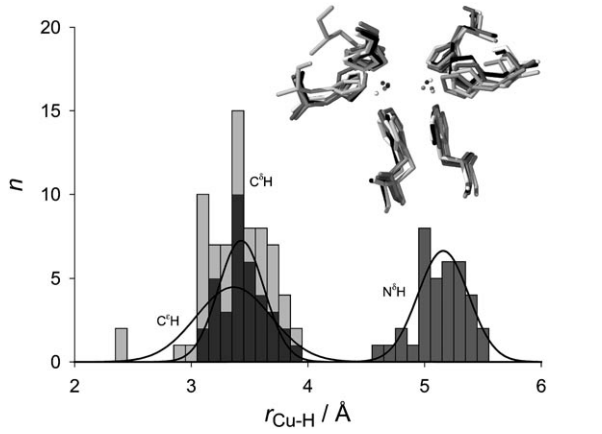

Figure 3. Copper to His proton distance distributions measured in the X-ray structures of several type-3 copper proteins ($C^{\delta}H$ dark grey, $C^{\varepsilon}H$ light grey, $N^{\delta}H$ grey). The solid lines represent best fits to the data using a Gaussian distribution function. An all-atom least-squares fit overlay of the used structures (see text) is shown in the upper right corner.

tion we selected the line widths of the well-resolved $Ty_{met}F$ CH signals (*b*, *i*, *j*, *k*, *l* in Figure 1A) at 600 MHz and 300 MHz as reported in Table 3. Based on the obtained τ_S

Table 3. T_2^{-1} (= R_2) values for the resolved $C^{\delta,\varepsilon}H$ signals in $Ty_{met}F$.

Signal	R_2 at 600 MHz [kHz]	R_2 at 300 MHz [kHz]	ΔR_2 [kHz]
b	1.54	0.93	0.61
i	1.05	0.74	0.31
j	0.92	0.58	0.34
k	1.05	0.57	0.48
l	1.11	0.66	0.45

values (see above), the experimental $-2J$ value, and r = 3.4 Å, it is possible to estimate the dipolar contributions to the transversal relaxation of the C^{δ} and C^{ε} protons by using Equation (3) (see Experimental Section). For $Ty_{met}F$, a value between 0.4 and 0.5 kHz is calculated for the dipolar contribution to T_2^{-1} ($=R_2$). Further, with a Cu–H distance of 3.4 Å, a τ_R value of 15–20 ns and 600 MHz field strength, a Curie contribution between 0.6 and 0.8 kHz to T_2^{-1} is calculated by using Equation (7) (see Experimental Section). Contact relaxation can be neglected for the C^{δ} and C^{ε} protons (20 Hz is calculated for T_{2cont}^{-1} using an A/h value of 1 MHz), but becomes sizeable for the N^{δ} protons, for which dipolar and Curie relaxation contribute less to the T_2^{-1} owing to their r^{-6} dependence. In the latter case, the relative contributions of dipolar, Curie, and contact relaxation to T_2^{-1} are more difficult to predict because of the uncertainty in the abovementioned ligand-centred contribution to the T_2^{-1}.

In this approximation, dipolar and Curie relaxation thus contribute about equally to the transverse relaxation rate of the C^{δ} and C^{ε} protons. Since Curie relaxation scales with the square of the magnetic field, a sharpening of signals is expected at lower field strength if the Curie mechanism contributes to T_2^{-1}. This is indeed observed. The T_2^{-1} values of $Ty_{met}F$ are significantly less at 300 MHz field strength, at which the average of the estimated T_2^{-1} values for the CH signals amounts to 0.7 kHz. The difference between the experimental line widths at 600 and 300 MHz amounts to 0.4 kHz, corresponding well with a ΔT_2^{-1} of 0.4–0.6 kHz, as calculated by using Equation (7) and the parameters given above.

Discussion

Based on paramagnetic NMR spectroscopy, enzyme kinetics and kinetics of fluoride binding,[3,19] we previously inferred that a single halide ion bridges the two copper ions in the active site of Ty_{met} and that it replaces the hydroxide molecule that is present in the native form.[3,19] The typical type-3 coordination geometry is maintained in all halide-bound species.[3]

Magnitude of the exchange coupling: The temperature dependence of the paramagnetic shifts could be fitted accurately to Equation (1). In $Ty_{met}F$ and $Ty_{met}Br$, the paramagnetic shift of one signal appeared not to follow the temperature dependence as predicted by Equation (1), possibly because of a structural rearrangement of the corresponding His residue with changing temperature.

Many attempts have been made to correlate the structural features of dinuclear copper complexes with the sign and magnitude of the magnetic exchange interaction, especially in relation with the nature and the coordination geometry of the bridging ligand (e.g.[33–35]). It appears that the Cu–X–Cu bridging angle is the most important parameter, with larger Cu–X–Cu bond angles leading to stronger antiferromagnetic coupling.[33–35] The $|-2J|$ value may vary over hundreds of wavenumbers in a group of related compounds with Cu–X–Cu bridging angles varying from about 100° to 125°. In the Ty_{met} species, we find a moderate to strong antiferromagnetic coupling with $-2J$ values following the order of $Ty_{met}F > Ty_{met}Cl > Ty_{met}Br$ (Table 1). By considering the radius of X^- when going down the halide group and assuming a constant Cu–Cu distance, the Cu–X–Cu angles would follow the order $F^- > Cl^- > Br^-$, thereby paralleling the experimental variation in $-2J$ values. The finding that $-2J$ depends on the nature of the halide ligand supports the proposed bridging mode of halide ions.

Spin density distribution: From EPR and ENDOR investigations of type-1 Cu sites combined with quantum chemical calculations it has been concluded that the amount of spin density present on the ligand histidines ranges from 5–10% per histidine.[36] The corresponding hyperfine interactions for the ring protons vary from 0.5 to 2 MHz,[37–40] similar to the values we find in the present case (Table 2). Since there are six histidine ligands in the active site of Ty this means that in Ty_{met} 1.4–1.7 spin density is present on the two copper ions and the atoms of the bridge. A difference between the spin density distribution over the His ligands in Ty and that in a type-1 site is that in the latter the hyperfine interaction decreases along the ring as the distance from the ligating nitrogen increases. In Ty the rings coordinate with their N^{ε}s but the hyperfine interaction for the adjacent CH protons is smaller than that for the N^{δ} proton, barring exceptions like His F in Figure 2B. Whether this difference is connected with differences in H-bonding pattern between the Cu sites in Ty and blue copper proteins needs further investigation.

Nuclear relaxation: The present data show that the paramagnetic longitudinal proton relaxation is dominated by the dipolar relaxation in all $Ty_{met}X$ derivatives. This means that T_1 data contain information on the distances from the copper to the resonating nucleus.

The line widths (i.e. T_2^{-1} s) instead consist of contributions from dipolar and Curie relaxation of similar magnitude. Since both relaxation mechanisms depend on the distance between the paramagnetic centre and the resonating nucleus

[Eqs. (3) and (7)], the line widths in the paramagnetic ^{1}H NMR spectra of the $Ty_{met}X$ species may serve as a qualitative indicator for the Cu–H distance.

Electronic relaxation: The paramagnetically shifted signals of proteins with a mononuclear Cu site are often too broad to be detectable owing to a long electronic relaxation time τ_S. In dinuclear Cu-containing *model compounds* an appreciable sharpening of the NMR signals has been observed, apparently because τ_S has shortened.[15] Our experiments show that a shortening of τ_S can also occur in *macromolecular* structures harbouring a type-3 centre.[9] The estimated τ_S values of the three Ty_{met} derivatives are on the order of 10^{-11} s and decrease according to $Ty_{met}F > Ty_{met}Cl > Ty_{met}Br$, as do the $-2J$ values.

The mechanism responsible for the shortening of τ_S has not been established. Fast electronic relaxation in Cu^{II} dimers may be due to the modulation of the zero-field splitting (ZFS) of the $S = 1$ level.[15,18] The modulation of the ZFS could arise from fluctuations in coordination geometry, collisions with solvent molecules, or molecular rotation. Still, even with fast relaxation between the sublevels of the $S = 1$ state, an additional fast relaxation between the $S = 0$ ground and the $S = 1$ excited state is needed to obtain (averaged) sharp paramagnetically shifted signals in the NMR spectrum. Actually, fast relaxation between the two states would be sufficient to get sharp paramagnetically shifted NMR lines. The density of phonon states in the 100–300 cm^{-1} range is likely to be sufficient for fast thermal relaxation between the triplet and singlet states. Relaxation may be further promoted by the extreme sensitivity of the $-2J$ splitting to the Cu-X-Cu angle. Thermal motion affecting this angle may provide an efficient time-dependent perturbation mechanism to enhance relaxation. Also, the spin-orbit coupling (SOC), which increases along the series F < Cl < Br, may help enhance relaxation. This would be in line with the observed decrease in τ_S along this series.

A similar mechanism involving electronic relaxation through a low-lying excited state has been suggested to explain the enhanced relaxation observed for the mixed-valence [Cu(1.5) Cu(1.5)] Cu_A sites of an engineered amicyanin[41] and cytochrome *c* oxidase[42] that also yield sharp NMR signals. In the Cu_A system, the energy difference between the electronic ground state MO ($^2B_{3u}$) and the first excited state MO ($^2B_{2u}$) is again on the order of a few 100 cm^{-1},[42] similar to the situation of Ty_{met}. The experimental τ_S values of the three $Ty_{met}X$ species are similar to the τ_S value reported for the Cu_A centre ($\tau_S \sim 10^{-11}$ s[41,42]).

Conclusion

In this study we have found that the properties of the $Ty_{met}X$ derivatives depend on the nature of the exchangeable Cu_2 bridging ligand. The $Ty_{met}X$ species are moderately antiferromagnetically coupled, with the experimental $-2J$ values following the same order as the expected Cu-X-Cu bridging angle in the $Ty_{met}X$ complexes.

Longitudinal relaxation is dipolar in origin, while the transversal relaxation arises from both the dipolar and the Curie relaxation. This implies that both T_1 and T_2 relaxation contain information on the distance of the copper to the resonating nucleus, a feature that may be used to study Ty_{met}-inhibitor complexes. It was further established that the relative sharpness of the signals in the $Ty_{met}X$ species is due to short electronic relaxation times that are different for each $Ty_{met}X$ species; the τ_S values follow the order of $Ty_{met}F > Ty_{met}Cl > Ty_{met}Br$ and lie around 10^{-11} s. Thus, previous conclusions that an efficient electronic relaxation mechanism in dimeric Cu^{2+} compounds may lead to relatively sharp NMR signals[9,15] can be extended to proteins containing a dinuclear type-3 Cu centre. The observed magnitude of the hyperfine coupling constants for the protons of the Cu-ligating histidine rings are compatible with 1.4–1.7 spins residing on the Cu_2 centre, including the bridging atoms.

Experimental Section

Protein isolation and purification: The enzyme was obtained from the growth medium of liquid cultures of *Streptomyces antibioticus* harbouring the pIJ703 Ty expression plasmid.[20,22] The protein was purified according to published procedures.[20] Purity was checked by SDS-PAGE and exceeded 95% in all preparations. Protein concentrations in pure samples were routinely determined optically using a value of 82 $mM^{-1}cm^{-1}$ for the extinction coefficient at 280 nm.[23]

Sample preparation and ^{1}H NMR measurements: NMR Ty_{met} samples (~0.6 mM in 100 mM NaPi at pH 6.80) were prepared as described before.[2] Samples recorded in H_2O contained 5% D_2O for the lock signal. ^{1}H spectra were recorded at 600 MHz or 300 MHz ^{1}H resonance frequency and at 4 °C using a Bruker DMX-600 or DPX-300 spectrometer with the use of the 180°-τ-90°-t_A super-WEFT pulse sequence,[24] an interpulse delay time of typically 55 ms and a 8 s^{-1} repetition rate. Depending on the required signal-to-noise ratio, 4,000 to 32,000 free induction decays were recorded and Fourier transformed using exponential apodization and a 60 Hz line-broadening function. The spectra were baseline corrected using the Bruker provided software. ^{1}H resonance T_1 values were measured by varying the interpulse delay time τ in the super-WEFT sequence using at least sixteen values for τ, where the signal intensities were measured using peak-heights. The estimated errors in the T_1 values are ±15%. Transversal relaxation rates R_2 (= T_2^{-1}) of resolved signals were determined from the resonance line widths by simulation of the signals using the line-fitting module implemented in the Mestre-C software (Cobas, J.C., Cruces, J. and Sardina, F.J., Universidad de Santiago de Compostela, Spain). The line widths obtained were corrected for the contribution introduced by the LB function, after which the R_2 values (in Hz) were calculated from the relation $R_2 = \pi\Delta\nu$ where $\Delta\nu$ denotes the line width at half-height.

Calculations: Values for $-2J$ were determined from the temperature dependence of ^{1}H chemical shifts using Equation (1):[16]

$$\delta_{con} = \frac{A_M}{T}\frac{g_e\mu_B}{\hbar\gamma_I k_B}\left(\frac{e^{(2J/k_BT)}}{1+3e^{(2J/k_BT)}}\right)\times 10^6 \quad (1)$$

in which δ_{con} represents the paramagnetic shift in ppm (equal to the observed shift δ_{obs} minus an assumed 8 ppm for the diamagnetic contribution), A_M is the isotropic electron–nucleus interaction energy,[25] g_e is the free electron *g*-value, μ_B is the Bohr magneton, $\hbar$ is Planck's constant divided by 2π, γ_I is the proton gyromagnetic ratio, k_B is the Boltzmann constant, $-2J$ is the singlet–triplet spacing energy, and T is the absolute temperature. The pseudocontact contribution to the paramagnetic shift is less than ten percent of the total shift in most cases[26] and is left out of con-

sideration. Similarly, a possible contribution from to the zero-field splitting in the triplet state is neglected.[27]

Dipolar, contact, and Curie relaxation rates were calculated by using Equations (2)–(9):[18]

$$T_{1\mathrm{dip}}^{-1} = \frac{2}{15}\left(\frac{\mu_0}{4\pi}\right)^2\left(\frac{\gamma_I^2 g_e^2 \mu_B^2}{r^6}\right)\left(\frac{7\tau_D}{1+\omega_S^2\tau_D^2}+\frac{3\tau_D}{1+\omega_I^2\tau_D^2}\right)P \quad (2)$$

$$T_{2\mathrm{dip}}^{-1} = \frac{1}{15}\left(\frac{\mu_0}{4\pi}\right)^2\left(\frac{\gamma_I^2 g_e^2 \mu_B^2}{r^6}\right)\left(4\tau_D+\frac{13\tau_D}{1+\omega_S^2\tau_D^2}+\frac{3\tau_D}{1+\omega_I^2\tau_D^2}\right)P \quad (3)$$

$$T_{1\mathrm{cont}}^{-1} = \frac{2}{3}\left(\frac{A_M}{\hbar}\right)^2\left(\frac{\tau_S}{1+\omega_S^2\tau_S^2}\right)P \quad (4)$$

$$T_{2\mathrm{cont}}^{-1} = \frac{1}{3}\left(\frac{A_M}{\hbar}\right)^2\left(\frac{\tau_S}{1+\omega_I^2\tau_S^2}+\tau_S\right)P \quad (5)$$

$$T_{1\mathrm{Cur}}^{-1} = \frac{2}{5}\left(\frac{\mu_0}{4\pi}\right)^2\left(\frac{\omega_I^2 g_e^4 \mu_B^4}{r_6(3k_BT)^2}\right)\left(\frac{3\tau_R}{1+\omega_I^2\tau_R^2}\right)2P \quad (6)$$

$$T_{2\mathrm{Cur}}^{-1} = \frac{1}{5}\left(\frac{\mu_0}{4\pi}\right)^2\left(\frac{\omega_I^2 g_e^4 \mu_B^4}{r_6(3k_BT)^2}\right)\left(4\tau_R+\frac{3\tau_R}{1+\omega_I^2\tau_R^2}\right)2P \quad (7)$$

with

$$\tau_D^{-1} = \tau_S^{-1}+\tau_R^{-1} \quad (8)$$

and

$$P = 1.5\exp\left(\frac{2J}{k_BT}\right)/\left[1+3\exp\left(\frac{2J}{k_BT}\right)\right] \quad (9)$$

In Equations (2)–(7), T_1 and T_2 are the longitudinal and transversal dipolar induced nuclear relaxation times, respectively, r is the distance from the resonating nucleus to the paramagnetic centre, μ_0 is the magnetic permeability of the vacuum, γ_I is the gyromagnetic ratio of the nucleus of interest, g_e is the free-electron g-value, μ_B is the Bohr magneton, ω_S and ω_I are the electronic and nuclear Larmor frequencies, respectively, τ_R is the rotational correlation time, and τ_S is the electronic relaxation time. Chemical exchange processes are too slow to contribute significantly to T_1^{-1} and T_2^{-1}.[16,28] The equations are based on the point–dipole approximation for the electronic magnetic moment.

Acknowledgements

The technical assistance of Cees Erkelens in the NMR measurements is gratefully acknowledged. The investigations were supported by the Netherlands Research Counsil for Chemical Sciences (NWO/CW project number 700–28–047).

[1] E. I. Solomon, U. M. Sundaram, T. E. Machonkin, *Chem. Rev.* **1996**, *96*, 2563–2605.
[2] L. Bubacco, J. Salgado, A. W. J. W. Tepper, E. Vijgenboom, G. W. Canters, *FEBS Lett.* **1999**, *442*, 215–220.
[3] A. W. J. W. Tepper, L. Bubacco, G. W. Canters, *J. Biol. Chem.* **2002**, *277*, 30436–30444.
[4] T. Klabunde, C. Eicken, J. C. Sacchettini, B. Krebs, *Nat. Struc. Biol.* **1998**, *5*, 1084–1090.
[5] M. E. Cuff, K. I. Miller, K. E. van Holde, W. A. Hendrickson, *J. Mol. Biol.* **1998**, *278*, 855–870.
[6] K. A. Magnus, B. Hazes, H. Ton-That, C. Bonaventura, J. Bonaventura, W. G. Hol, *Protein J.* **1994**, *19*, 302–309.
[7] A. Volbeda, W. G. Hol, *J. Mol. Biol.* **1989**, *209*, 249–279.
[8] *NMR of Paramagnetic Molecules, Principles and Applications* (Eds.: G. N. La Mar, W. Horrocks Jr., R. H. Holm), Academic Press, New York, **1973**.
[9] R. C. Holz, M. L. Alvarez, W. G. Zumft, D. M. Dooley, *Biochemistry* **1999**, *38*, 11164–11171.
[10] A. Asokan, P. T. Manoharan, *Inorg. Chem.* **1999**, *38*, 5642–6554.
[11] J. M. Brink, R. A. Rose, R. C. Holz, *Inorg. Chem.* **1996**, *35*, 2878–2885.
[12] W. Byers, R. J. P. Williams, *J. Chem. Soc. Dalton* **1973**, 555–560.
[13] M. Maekawa, S. Kitagawa, M. Munakata, H. Masuda, *Inorg. Chem.* **1989**, *28*, 1904–1909.
[14] R. A. Zelonka, M. C. Baird, *Inorg. Chem.* **1972**, *11*, 134.
[15] N. N. Murthy, K. D. Karlin, I. Bertini, C. Luchinat, *J. Am. Chem. Soc.* **1997**, *119*, 2156–2162.
[16] I. Bertini, C. Luchinat, *Coord. Chem. Rev.* **1996**, *150*.
[17] I. Bertini, O. Galas, C. Luchinat, G. Parigi, G. Spina, *J. Magn. Reson.* **1998**, *130*, 33–44.
[18] V. Clementi, C. Luchinat, *Acc. Chem. Res.* **1997**, *30*, 351–361.
[19] A. W. Tepper, L. Bubacco, G. W. Canters, *J. Biol. Chem.* **2003**, *279*, 13425–13435.
[20] L. Bubacco, E. Vijgenboom, C. Gobin, A. W. J. W. Tepper, J. Salgado, G. W. Canters, *J. Mol. Catal. B* **2000**, *6*, 27–35.
[21] A. W. J. W. Tepper, L. Bubacco, G. W. Canters, *J. Am. Chem. Soc.* **2005**, *127*, 567–575.
[22] E. Katz, C. J. Thompson, D. A. Hopwood, *J. Gen. Microbiol.* **1983**, *129*, 2703–2714.
[23] M. P. Jackman, A. Hajnal, K. Lerch, *Biochem. J.* **1991**, *274*, 707–713.
[24] T. Inubushi, E. D. Becker, *J. Magn. Reson.* **1983**, *51*, 128–133.
[25] A_M represents the isotropic hyperfine interaction between nucleus and unpaired electron in the absence of exchange coupling between the unpaired electrons on the two copper ions.[16] When the hyperfine interaction is defined as $A\,\boldsymbol{I}.\boldsymbol{S}_t$ *in which* $\boldsymbol{S}_t = \boldsymbol{S}_1 + \boldsymbol{S}_2$,[2] A_M should be replaced by $2A$ in Equation (1).[2]
[26] The pseudocontact shift δ_{pc} is given by Equation (10):[43]

$$\delta_{pc} = \frac{\beta^2 S(S+1)}{9k_BT}\left(g_\parallel^2 - g_\perp^2\right)\frac{1}{r^3}\left(3\cos^2\theta - 1\right)P \quad (10)$$

θ is the angle between the z axis of the g tensor and the vector connecting the nucleus with the electronic dipole, the other symbols have their usual meaning. For Cu_2 model compounds, the anisotropy in the g tensor amounts to less than 10%, which leads to $(g_\parallel^2 - g_\perp^2) \approx 0.4$.[43]–[46] The shift δ_{pc} was calculated for the protons of the six histidines in the activate site of *Limulus polyphemus* hemocyanin (PDB 1OXY) and catechol oxidase from *Ipomoea batatas* (PDB 1BT3) by placing a magnetic dipole ($S = {}^1/_2$) on each of the two Cu centres and averaging their contributions (see Table S1 in the Supporting Information). For only two out of the 18 protons, $|\delta_{pc}|$ amounts to about 4 ppm, while for almost all other cases $|\delta_{pc}|$ is <2 ppm.
[27] The zero-field splitting in the triplet state may contribute to the pseudo-contact shift.[16] The dipolar interaction in a Cu_2 pair with the coppers 2.5 Å apart contributes 0.1 cm^{-1} to the zero-field splitting parameter D in Cu_2 model compounds.[44] The spin-orbit coupling is not expected to contribute appreciably either. In agreement with this, common values for D are in the range of 0.2–2 cm^{-1} (e.g. refs. [44]–[48]), which is small relative to the Zeeman energy in a 14 T field and small relative to k_BT. Thus, the contribution to δ_{pc} is predicted to be negligible.[16]
[28] From NMR and kinetic experiments on halide binding to Ty_{met}, it has been found that halide-free Ty_{met} and halide-bound Ty_{met} are in slow exchange on the NMR time scale (the measured k_{off} of the Cu_2 bridging F^- amounts to 14 s^{-1} at pH 6.8[19]). The effects of the slow halide exchange on the relaxation character of the His protons in the active site are therefore negligible. Vibrations in the active site may modulate the electronic interaction but not the electron-nucleus interaction to any appreciable extent. They may affect the electron but not the nuclear-spin relaxation (vide infra).
[29] A. Asokan, B. Varghese, P. T. Manoharan, *Inorg. Chem.* **1999**, *38*, 4393–4399.
[30] P. K. Mandaln, P. T. Manoharan, *Inorg. Chem.* **1995**, *34*, 270–277.
[31] The relative importance of the contact and dipolar contributions to the T_1^{-1} can be easily estimated with the help of Equations (2) and (4). Typical values for the interaction matrix elements are $A_M/h =$

9 Mrad s^{-1} (Table 1), and $(\gamma_I g \mu_B)/r^3 \approx 9$ Mrad s^{-1} ($r = 4$ Å). Thus, the matrix elements for the contact and the dipolar interactions are of the same order. For evaluating the spectral density parts in Equation (4) it should be realised that $\tau_D \approx \tau_S$ and that $\omega_S \tau_S \gg 1$, while $\omega_I \tau_S \ll 1$. Consequently, the spectral density part in Equations (2) and (4) reduce to $3\tau_S$ and that $\tau_S/\omega_S{}^2\tau_S{}^2$ ($\ll \tau_S$), respectively. Therefore, the T_1 is dominated by the dipolar interaction in the present case.

[32] The extent of the approximation can be estimated by considering that τ_S is calculated from the $T_1{}^{-1}$ by the use of Equation (2), which simplifies, in the present case, to Equation (11):

$$T_{1D}^{-1} = \tfrac{2}{5}\left(\tfrac{\mu_0}{4\pi}\right)^2 \left(\tfrac{\gamma_I g_e \mu_B}{r^3}\right)^2 \tau_S P \qquad (11)$$

Here, the electron spin density is equally divided over the two copper ions and only the interaction with the nearest copper is taken into account.[16] A more precise approximation incorporates the following corrections: 1) The spin density on the second Cu atom, although farther away, contributes an estimated 10–40 % to the interaction matrix element (see also Table S1 in the Supporting Information). 2) Delocalisation of the spin over the His ligands decreases the spin density on the coppers by 15–30 %, leading to a corresponding decrease in the dipolar interaction. 3) About 0.05 to 0.1 spin density resides on average on each of the six His ligands. The dipolar interaction of, for instance, one percent of spin density on a ring carbon atom with the adjacent proton at about 1.1 Å may contribute another 10–30 % to the dipolar interaction term. In conclusion, the actual value for τ_S may be *shorter* than quoted in Table 1 by a factor of 1.2 to 2.5.

[33] M. Rodriguez, A. Llobet, M. Corbella, A. E. Martell, J. Reibenspies, *Inorg. Chem.* **1999**, *38*, 2328–2334.

[34] S. S. Tandon, L. K. Thompson, M. E. Manuel, J. N. Bridson, *Inorg. Chem.* **1994**, *33*, 5555–5570.

[35] L. K. Thompson, S. K. Mandal, S. S. Tandon, J. N. Bridson, M. K. Park, *Inorg. Chem.* **1996**, *35*, 3117–3125.

[36] J. W. A. Coremans, O. G. Poluektov, E. J. J. Groenen, G. W. Canters, H. Nar, A. Messerschmidt, *J. Am. Chem. Soc.* **1996**, *118*, 12141–12153.

[37] A. P. Kalverda, J. Salgado, C. Dennison, G. W. Canters, *Biochemistry* **1996**, *35*, 10586.

[38] A. P. Kalverda, J. Salgado, C. Dennison, G. W. Canters, *Biochemistry* **1996**, *35*, 3085–3092.

[39] I. Bertini, C. O. Fernandez, B. G. Karlsson, J. Leckner, C. Luchinat, B. G. Malmstrom, A. M. Nersissian, R. Pierattelli, E. Shipp, J. S. Valentine, A. J. Vila, *J. Am. Chem. Soc.* **2000**, *122*, 3701–3707.

[40] U. Kolczak, J. Salgado, G. Siegal, M. Saraste, G. W. Canters, *Biospectroscopy* **1999**, *5*, S19-S32.

[41] C. Dennison, A. Berg, G. W. Canters, *Biochemistry* **1997**, *36*, 3262–3269.

[42] J. Salgado, G. Warmerdam, L. Bubacco, G. W. Canters, *Biochemistry* **1998**, *37*, 7378–7389.

[43] R. A. Dwek, *NMR in Biochemistry*, Oxford University Press, London, **1973**.

[44] L. Gutierrez, G. Alzuet, J. Borras, A. Castineiras, A. Rodriguez-Fortea, E. Ruiz, *Inorg. Chem.* **2001**, *40*, 3089–3096.

[45] K. J. Oberhausen, J. F. Richardson, R. M. Buchanan, J. K. Mccusker, D. N. Hendrickson, J. M. Latour, *Inorg. Chem.* **1991**, *30*, 1357–1365.

[46] H. M. J. Hendriks, P. J. M. W. Birker, G. C. Verschoor, J. Reedijk, *J. Chem. Soc. Dalton Trans.* **1982**, 623–631.

[47] C. F. Martens, A. P. H. J. Schenning, M. C. Feiters, J. Heck, G. Beurskens, P. T. Beurskens, E. Steinwender, R. J. M. Nolte, *Inorg. Chem.* **1993**, *32*, 3029–3033.

[48] H. W. Richardson, J. R. Wasson, W. E. Hatfield, *J. Mol. Struct.* **1977**, *36*, 83–91.

Received: December 1, 2005
Revised: April 12, 2006
Published online: July 6, 2006

